Digital Self-Interference Cancellation for Full-Duplex Underwater Acoustic Systems

Lu Shen, *Student Member, IEEE*, Benjamin Henson, *Member, IEEE*,
Yuriy Zakharov, *Senior Member, IEEE*, Paul Mitchell, *Senior Member, IEEE*

***Abstract*—Underwater acoustic (UWA) communication suffers from the limited available bandwidth for data transmission. Full-duplex (FD) communication has demonstrated the ability of achieving high spectral efficiency in terrestrial radio communications. There is a significant potential in adopting the benefits of FD in UWA systems. The major obstacle in FD communications is the severe self-interference (SI) introduced by the near-end transmitted signal. For FD UWA communications, the low signal frequency allows high-resolution ADCs to be used. With higher performance ADCs, it might be possible to achieve higher digital SI cancellation performance than that in FD radio systems. In this paper, we present experimental results of digital SI cancellation in FD UWA system, based on the use of the low-complexity recursive least-squares (RLS) adaptive filter with dichotomous coordinate descent iterations. The experimental results demonstrate that up to 46 dB of SI is cancelled when we use the transmitted digital data as the regressor in the adaptive filter. To improve the SI cancellation performance without introducing high-complexity operation, we use the digitalized power amplifier (PA) output as the regressor to deal with the non-linear distortions caused by the PA in the transmitted chain. With this technique, as high a level as 69 dB of digital SI cancellation is achieved.**

***Index Terms*—Digital cancellation, full-duplex, self-interference, underwater acoustic communications.**

I. Introduction

ACOUSTIC communications is the only feasible technology for long-range underwater data transmission. However, the available frequency bandwidth is very limited [1], [2]. To maximise the capacity of the acoustic links, we consider full-duplex (FD) communications, when a transceiver simultaneously transmits and receives data in the same frequency band [3]–[5]. The main challenge of achieving FD communication is the strong self-interference (SI) introduced by the near-end transmission [6]–[11]. Due to the high transmission power of the near-end data, we expect to deal with a high level of SI, which can be 100 dB higher than the noise floor in some communication scenarios. The residual SI will reduce the signal to noise ratio (SNR) of the desired signal and thus will degrade the system performance.

It is widely believed in FD terrestrial radio communications that digital cancellation alone is not sufficient for SI cancellation due to the limitation of the analogue-to-digital converter (ADC) [6], [7], [12]. The maximum achievable digital SI cancellation is determined by the dynamic range of the ADC [13]–[16]. In general, significantly lower frequencies are used in UWA communications compared to those used in terrestrial radio communications. In such a case, ADCs up to 24 bits are available, which would allow digital cancellation of 100 dB to be feasible. As demonstrated in [6], [7], around 30 dB of SI cancellation can be achieved with digital cancellation. In those designs, the non-linear distortion introduced by the power amplifier (PA) is not included in the channel model which limits the cancellation performance. Subsequent designs address the non-linear SI by either using two-step digital cancellation (cancel the linear and non-linear SI components separately) [13] or by developing a non-linear adaptive filter [17]. These designs obtain up to 48 dB of digital SI cancellation at the expense of high complexity [13], [17], [18].For FD UWA systems, a combination of digital and analogue cancellation is considered in [19]. This design achieves around 30 dB of digital SI cancellation with a multipath SI channel model. The recent work [11] proposes a sparse adaptive algorithm for estimation of the SI channel and PA nonlinearity, but the cancellation performance is limited. One approach to dealing with the PA nonlinearity without developing a high complexity digital SI canceller is to use the PA output as a reference signal [20]. In such a case, a linear canceller can be sufficient. In [20], this idea is investigated by simulation for multi-carrier communication signals.

Here we present a low-complexity practical digital SI canceller for FD UWA systems, which achieves a significantly higher level of SI cancellation compared to reported experimental results for terrestrial radio and UWA systems. Our design uses the PA output to reduce the effect of the PA nonlinearity on the SI performance. We implement this idea for single-carrier communication signals. The cancellation is based on reconstruction of the SI signal using a SI channel estimate obtained by a low-complexity recursive least-squares (RLS) adaptive filter with dichotomous coordinate descent (DCD) iterations [21], [22]. We present results of experiments conducted in an indoor water tank. The experimental results show that the proposed design can achieve as high SI cancellation as 69 dB, which is 23 dB higher than that achieved by an architecture with the digital data as the reference signal.

II. System Model

The FD system model is shown in Fig. 1. The system operates at two sampling rates. The high sampling rate f_s is used for both the near-end data transmission and generation of the received digital samples. The lower sampling rate f_d is

The authors are with Department of Electronic Engineering, University of York, U.K. (e-mail: ls1215@york.ac.uk; benjamin.henson@york.ac.uk; yury.zakharov@york.ac.uk; paul.mitchell@york.ac.uk).

The work of B. Henson, Y. Zakharov and P. Mitchell was supported in part by the U.K. EPSRC through Grants EP/P017975/1 and EP/R003297/1.

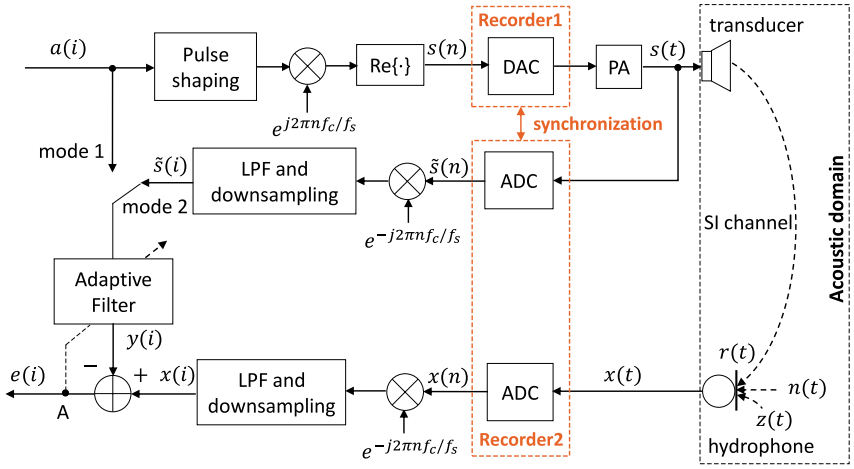

Fig. 1: Block diagram of the FD UWA system model.

used for SI channel estimation and digital cancellation. The sample index with the high sampling rate f_s and the low sampling rate f_d are denoted by n and i, respectively; e.g, the transmitted signal $s(t)$ sampled at f_s is denoted as $s(n)$.

We consider transmitting a pseudo-random sequence of complex data symbols $a(i)$. The transmitted data is up-sampled from f_d to f_s, pulse-shape filtered and up-converted to the carrier frequency f_c. The root-raised cosine (RRC) filter is used for the pulse-shaping [24]. Then, the passband signal $s(n)$ is digital-to-analogue converted (DAC), amplified in the PA and transmitted by a transducer. The SI channel output $r(t)$ along with the far-end desired signal $z(t)$ and the noise $n(t)$ are received by the near-end hydrophone. The far-end signal $z(t)$ is transmitted over the same frequency band as the near-end transmission. Note that the far-end signal introduces additional interference at the hydrophone, that degrades the SI channel estimation performance. Since the aim of this paper is to obtain the baseline performance of the digital SI cancellation, so far the far-end signal is not considered in the experiments.

We use an adaptive filter for SI channel estimation and SI signal reconstruction. As shown in Fig. 1, the system can switch between two modes. In mode 1, the transmitted digital data $a(i)$ is used as the regressor in the adaptive filter. In mode 2, we use baseband samples $\tilde{s}(i)$ of the analogue output $s(t)$ of the PA as the regressor. After the ADC, the digitalized PA output is down-converted, low-pass filtered (LPF) by an RRC filter and downsampled to f_d before being used as the adaptive filter input. The received signal $x(t)$ undergoes the same front-end processing as the analogue PA output $s(t)$ before being used as the desired signal $x(i)$ in the adaptive filter [23]. The downsampling of the input signal before the adaptive filtering is used to reduce the computational complexity and to avoid the ill-condition problem caused by a high condition number of the autocorrelation matrix of the narrowband regressor [23].

In practice, the SI channel is not static due to the time-varying sea environment. Apart from the direct SI path between the transducer and the hydrophone, there are reflections from the moving sea surface, with typical periods from 5 s to 20 s [25]. Thus, fast convergence speed is one of the main features we are interested in. On the other hand, one of our objectives is practical implementation of the SI cancellation algorithm on a real-time design platform, such as a DSP board [26]. Therefore, the computational complexity and numerical stability are also crucial factors for algorithm selection.

The fastest convergence is achieved by the classical RLS algorithm, but it suffers from numerical instability and possesses high computational complexity. The numerical instability is a consequence of the recursive matrix inversion. This recursion allows a reduced complexity of $\mathcal{O}(L^2)$ arithmetic operations per sample, which however is still too high for practical implementation.

We use the RLS-DCD algorithm that has a convergence speed comparable to that of the classical RLS algorithm, it is numerically stable and has a significantly lower complexity [21]. Moreover, the RLS-DCD algorithm is well suited to implementation in fixed-point arithmetic, in particular, in hardware [21], [22]. Instead of the matrix inversion, it solves a system of normal equations, thus making the algorithm numerically stable. For the solution, it uses DCD iterations. Its impulse response is only updated for each successful DCD iteration, in which the cost function is reduced. The overall complexity of the RLS-DCD algorithm is $\mathcal{O}(LN_u)$ operations per sample, where N_u is the number of DCD updates, and $N_u \ll L$. With $N_u = 2$, as is in our experiments, the complexity of the RLS-DCD algorithm is comparable with that of the normalized least mean squares (NLMS) adaptive filter, considered to be one of the least complicated algorithms [22].

III. Experimental Setup

In our experiment, We transmit BPSK symbols at the carrier frequency $f_c = 12$ kHz. The symbol rate is $f_d = 1$ kHz. The RRC roll-off factor is 0.2 and the filter length is of a duration of 14 symbols (14 ms). A Hanning window is applied to the

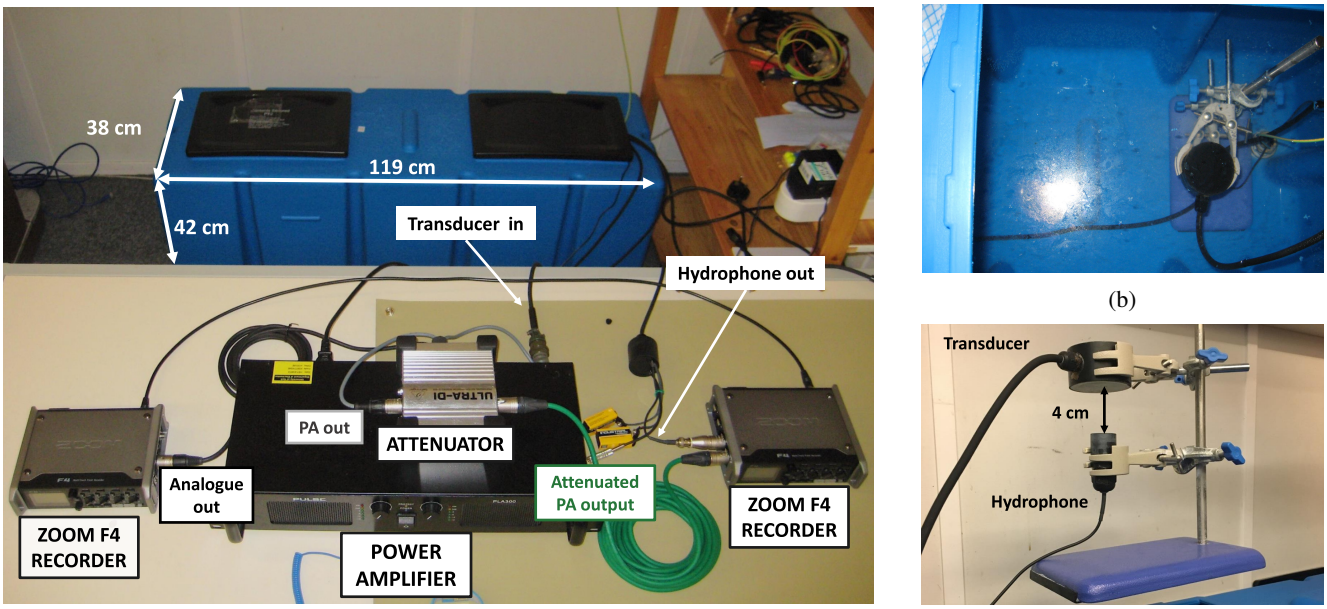

Fig. 2: (a) Experimental setup of the FD UWA system; (b) Vertical view of the tank; (c) Placement of the transducer and hydrophone underwater.

filter coefficients to avoid the edge effects due to the truncation of the RRC impulse response. The length of the transmitted signal is 15s, which includes 5s of zero padding before the data transmission. The received signal during this silence period is used to measure the background noise in the water tank.

The experiments are conducted in a $38 \times 119 \times 42\,\mathrm{cm}^3$ plastic water tank filled with 120 litres of water. Fig. 2(a) shows the experimental setup. We use a Benthowave BII-7530 transducer [27] for the near-end data transmission and a Benthowave BII-7010 hydrophone [28] for the SI reception. As shown in Fig. 2(b) and (c), the transducer and hydrophone are clamped by a retort stand with a fixed distance between them of 4 cm and submerged in the water during the experiment. In Fig. 3, a snapshot of the SI channel estimate in the water tank is plotted. This channel estimate represents the adaptive filter taps after convergence of the RLS-DCD algorithm in the second (more accurate) mode. It can be seen that we have a long impulse response with a delay spread of around 80 ms, which is considered to be typical for UWA communications [29].

The passband digital samples $s(n)$ of the transmitted signal are generated in MATLAB and stored in an SD card of the Zoom F4 multitrack recorder [30]. This recorder converts these samples to an analogue signal with a 24-bit DAC and passes it to the PULSE PLA300 PA [31]. Finally, the amplified analogue signal is fed to the transducer and transmitted.

As mentioned in Section II, the system has two modes of digital cancellation. The second mode requires access to the PA output to generate the regressor for the adaptive filter. The hydrophone output and PA output are recorded during the experiment. The recording device contains a high resolution 24-bit ADC to avoid introducing high quantization

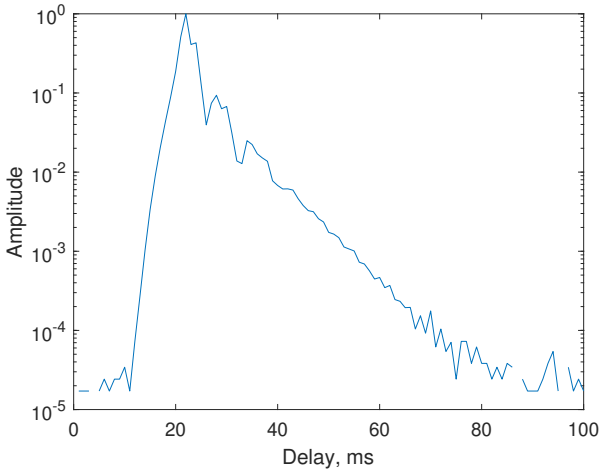

Fig. 3: Impulse response estimate of the SI channel.

noise. In our experiments, we record the PA output and the hydrophone output using another Zoom F4 multitrack recorder at a sampling rate of 96 kHz. Although we use the same type and model of recorders for data transmission and reception, the sampling rates generated by the two oscillators in the recorders might not be identical. Thus, we have synchronized the audio clock of the two recorders to avoid a difference between the sampling rates in the transmit and receive chains.

Due to the high voltage level of the PA output (up to 48 V in our experiments), the PA output is attenuated by the Behringer DI100 attenuator [32] before being fed to the recorder.

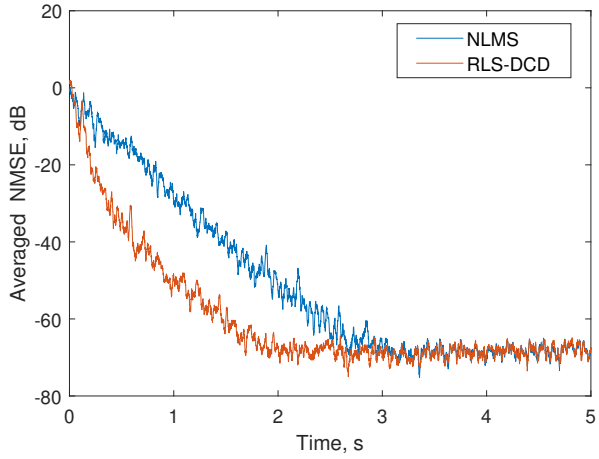

Fig. 4: Averaged NMSE performance of the NLMS and RLS-DCD algorithms.

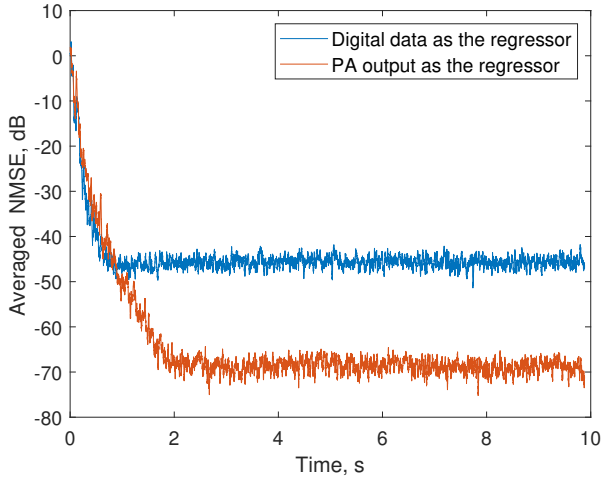

Fig. 5: Averaged NMSE performance in the two cancellation modes.

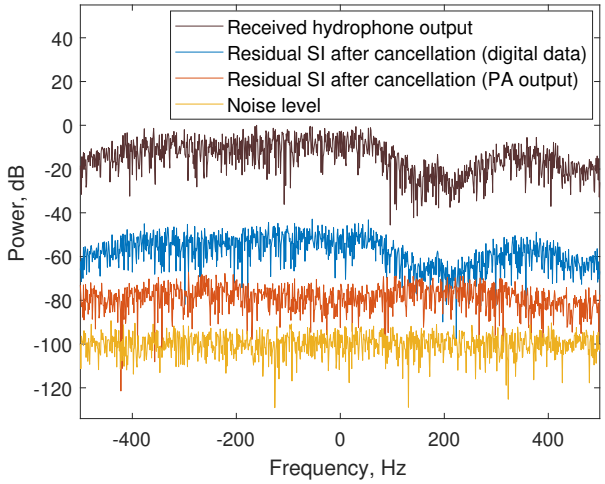

Fig. 6: Power spectra of the received signal before and after the digital cancellation.

IV. Experimental Results

In this section, the experimental results of digital SI cancellation in the FD UWA system are presented. The SI cancellation performance is evaluated by the steady-state normalized mean-squared error (NMSE) level of the adaptive filter, which is computed as:

$$\text{steady-state NMSE} = \frac{\mathrm{E_e}}{\mathrm{E_x}} = \frac{\mathbf{e}^H\mathbf{e}}{\mathbf{x}^H\mathbf{x}},$$

where E_e is the energy of the error vector $\mathbf{e} = [e(M), \ldots, e(i), \ldots, e(N)]^T$, $\mathbf{e}^H$ is the Hermitian transpose of $\mathbf{e}$, E_x is the energy of the vector $\mathbf{x} = [x(M), \ldots, x(i), \ldots, x(N)]^T$ of the desired signal $x(i)$ in the adaptive filter, N is the total number of samples in the error signal, M indicates the start of the steady-state of the RLS-DCD algorithm. Specifically, the steady-state NMSE level is computed from 5s to about 10s of the received signal after the silence period.

In Fig. 4, we show the NMSE performance of the NLMS and RLS-DCD algorithms in the second mode. The filter length is $L = 100$. The algorithm parameters are tuned to achieve the same steady-state NMSE level. The NLMS step-size is $\mu = 0.3$. For the RLS-DCD algorithm, the forgetting factor $\lambda = 1 - 1/4L = 0.9975$, the number of bits representing the impulse response $M_b = 16$, and the number of updates N_u = 2 [21]. The NMSE curves are smoothed by averaging the instantaneous NMSE over a period of 15 ms, to provide a better vision of the NMSE performance for comparison. The RLS-DCD algorithm clearly shows a faster convergence speed than the NLMS algorithm.

In Fig. 5, we compare the digital SI cancellation performance in the two modes. In each mode, a delay is adjusted and applied to the regressor to ensure the whole channel delay spread is covered by the adaptive filter length. From our investigation, a filter length of $L = 100$ taps is sufficient for capturing the whole channel delay spread in the water tank. Parameters of the RLS-DCD algorithm are the same as we used for NMSE performance comparison. With the aforementioned parameters, we achieve the same steady-state NMSE level as the classical RLS algorithm (not shown here). The NMSE curves are again smoothed in the same way to provide a clearer vision. As shown in Fig. 5, when we use the digital data as the regressor, the steady-state NMSE level is close to -46 dB, which is remarkably good. However, the NMSE level can be further reduced to -69 dB with the PA output being used as the regressor. This amount of digital SI cancellation is significantly higher than that achieved in the FD terrestrial radio communications.

The spectra of the received signal before and after digital cancellation are shown in Fig. 6. Both the NMSE performance and the signal spectra demonstrate that the digital cancellation when using the PA output as the regressor significantly outperforms that with the digital data. We believe that the observed 23 dB improvement in SI cancellation in the second mode is achieved by taking into account the non-linear distortions introduced by the PA.

It can be seen in Fig. 6 that the residual signal after digital cancellation is still 20 dB higher than the noise floor. This can

be attributed to the residual non-linear distortions introduced by other equipment rather than the PA. The transducer and the hydrophone only exhibit a linear mechanical response for small amplitudes [33]. There will therefore be non-linear components present during the data transmission and reception. Likewise, the hydrophone we use has an integrated pre-amplifier. The pre-amplifier will certainly introduce extra non-linear distortion to the received signal which is not taken into account with a linear adaptive filter.

V. Conclusions and Future work

In this paper, we have presented the digital SI cancellation performance of an FD UWA system based upon tank experimental data. The RLS-DCD adaptive filtering algorithm is used for digital SI cancellation due to its fast convergence speed, numerical stability and low computational complexity. The digital SI cancellation performance in the FD UWA system is presented and compared by using two different signals as the regressor. The experimental results show that up to 69 dB of SI can be cancelled with the PA output being used as the regressor in the adaptive filter, which outperforms by 23 dB the cancellation performance with the digital data.

As future work, we will introduce the far-end signal to the receiver to establish a complete setup of the FD UWA system. The far-end signal will be acting as an extra interference for SI estimation at the receiver, which should reduce the SI cancellation performance. Therefore, we will operate joint estimation of the SI channel and the far-end signal with turbo iterations. Such an approach would allow us to eliminate the influence of the far-end signal on the SI channel estimation performance. In such a case, we would be able to approach the SI cancellation performance as presented in this paper.

References

[1] I. F. Akyildiz, D. Pompili, and T. Melodia, "Underwater acoustic sensor networks: Research challenges," *Ad Hoc Networks*, vol. 3, no. 3, pp. 257–279, 2005.

[2] T. H. Eggen, A. B. Baggeroer, and J. C. Preisig, "Communication over Doppler spread channels. Part I: Channel and receiver presentation," *IEEE Journal of Oceanic Engineering*, vol. 25, no. 1, pp. 62–71, 2000.

[3] D. Bliss, P. Parker, and A. Margetts, "Simultaneous transmission and reception for improved wireless network performance," in *IEEE 14th Workshop on Statistical Signal Processing*, 2007, pp. 478–482.

[4] B. Radunovic, D. Gunawardena, P. Key, A. Proutiere, N. Singh, V. Balan, and G. Dejean, "Rethinking indoor wireless mesh design: Low power, low frequency, full-duplex," in *IEEE 5th Workshop on Wireless Mesh Networks*, 2010, pp. 1–6.

[5] G. Qiao, S. Liu, Z. Sun, and F. Zhou, "Full-duplex, multi-user and parameter reconfigurable underwater acoustic communication modem," in *MTS/IEEE Oceans - San Diego*, 2013, pp. 1–8.

[6] M. Duarte and A. Sabharwal, "Full-duplex wireless communications using off-the-shelf radios: Feasibility and first results," in *44th Asilomar Conference on Signals, Systems and Computers*, 2010, pp. 1558–1562.

[7] J. I. Choi, M. Jain, K. Srinivasan, P. Levis, and S. Katti, "Achieving single channel, full duplex wireless communication," in *16th Annual International Conference on Mobile Computing and Networking*, 2010, pp. 1–12.

[8] E. Everett, M. Duarte, C. Dick, and A. Sabharwal, "Empowering full-duplex wireless communication by exploiting directional diversity," in *45th Asilomar Conference on Signals, Systems and Computers*, 2011, pp. 2002–2006.

[9] B. King, J. Xia, and S. Boumaiza, "Digitally assisted RF-analog self interference cancellation for wideband full-duplex radios," *IEEE Transactions on Circuits and Systems II: Express Briefs*, vol. 65, no. 3, pp. 336–340, 2018.

[10] J. Zhou and H. Krishnaswamy, "A system-level analysis of phase noise in full-duplex wireless transceivers," *IEEE Transactions on Circuits and Systems II: Express Briefs*, vol. 65, no. 9, pp. 1189–1193, 2018.

[11] G. Qiao, S. Gan, S. Liu, L. Ma, and Z. Sun, "Digital self-interference cancellation for asynchronous in-band full-duplex underwater acoustic communication," *Sensors*, vol. 18, no. 6, pp. 1700–1716, 2018.

[12] M. Duarte, C. Dick, and A. Sabharwal, "Experiment-driven characterization of full-duplex wireless systems," *IEEE Transactions on Wireless Communications*, vol. 11, no. 12, pp. 4296–4307, 2012.

[13] D. Bharadia, E. McMilin, and S. Katti, "Full duplex radios," in *ACM SIGCOMM Computer Communication Review*, vol. 43, no. 4, 2013, pp. 375–386.

[14] L. Anttila, D. Korpi, V. Syrjala, and M. Valkama, "Cancellation of power amplifier induced nonlinear self-interference in full-duplex transceivers," in *47th Asilomar Conference on Signals, Systems and Computers*, 2013, pp. 1193–1198.

[15] D. Korpi, T. Riihonen, V. Syrjälä, L. Anttila, M. Valkama, and R. Wichman, "Full-duplex transceiver system calculations: Analysis of ADC and linearity challenges," *IEEE Transactions on Wireless Communications*, vol. 13, no. 7, pp. 3821–3836, 2014.

[16] T. Riihonen and R. Wichman, "Analog and digital self-interference cancellation in full-duplex MIMO-OFDM transceivers with limited resolution in A/D conversion," in *46th Asilomar Conference on Signals, Systems and Computers*, 2012, pp. 45–49.

[17] D. Korpi, Y. S. Choi, T. Huusari, L. Anttila, S. Talwar, and M. Valkama, "Adaptive nonlinear digital self-interference cancellation for mobile inband full-duplex radio: Algorithms and RF measurements," in *IEEE Global Communications Conference*, 2015, pp. 1–7.

[18] M. Emara, P. Rosson, K. Roth, and D. Dassonville, "A full duplex transceiver with reduced hardware complexity," in *IEEE Global Communications Conference*, 2017, pp. 1–6.

[19] L. Li, A. Song, L. J. Cimini, X. G. Xia, and C. C. Shen, "Interference cancellation in in-band full-duplex underwater acoustic systems," in *MTS/IEEE Oceans - Washington*, 2015, pp. 1–6.

[20] S. Li and R. D. Murch, "An investigation into baseband techniques for single-channel full-duplex wireless communication systems," *IEEE Transactions on Wireless Communications*, vol. 13, no. 9, pp. 4794–4806, 2014.

[21] Y. V. Zakharov, G. P. White, and J. Liu, "Low-complexity RLS algorithms using dichotomous coordinate descent iterations," *IEEE Transactions on Signal Processing*, vol. 56, no. 7, pp. 3150–3161, 2008.

[22] J. Liu, Y. V. Zakharov, and B. Weaver, "Architecture and FPGA design of dichotomous coordinate descent algorithms," *IEEE Transactions on Circuits and Systems I: Regular Papers*, vol. 56, no. 11, pp. 2425–2438, 2009.

[23] S. Haykin, *Adaptive Filter Theory*. Prentice Hall, 2002.

[24] J. Proakis and M. Salehi, *Digital Communications*, ser. McGraw-Hill International Edition. McGraw-Hill, 2008.

[25] N. M. Shapiro, M. Campillo, L. Stehly, and M. H. Ritzwoller, "High-resolution surface-wave tomography from ambient seismic noise," *Science*, vol. 307, no. 5715, pp. 1615–1618, 2005.

[26] "ANALOG DEVICES Datasheet of the SHARC+ Dual-Core DSP with Arm Cortex-A5," [Accessed: 30- Jan- 2019]. [Online]. Available: https://www.analog.com/media/en/technical-documentation/data-sheets/ADSP-SC582_583_584_587_589_ADSP-21583_584_587.pdf

[27] "Low frequency underwater transducer," [Accessed: 08- Oct- 2018]. [Online]. Available: https://www.benthowave.com/products/BII-7530lowfrequencytransducer.html.

[28] "Low noise broadband hydrophone," [Accessed: 19- Nov- 2018]. [Online]. Available: https://www.benthowave.com/products/BII-7010Hydrophone.html.

[29] M. Stojanovic and J. Preisig, "Underwater acoustic communication channels: Propagation models and statistical characterization," *IEEE communications magazine*, vol. 47, no. 1, pp. 84–89, 2009.

[30] "Zoom F4 multitrack recorder," [Accessed: 08- Oct- 2018]. [Online]. Available: https://www.zoom-na.com/products/field-video-recording/field-recording/zoom-f4-multitrack-field-recorder.

[31] "Pulse PLA series Power Amplifier," [Accessed: 16- Nov- 2018]. [Online]. Available: http://www.pulse-audio.co.uk/product/pla300/

[32] "ULTRA-DI DI100 Professional Battery/Phantom Powered DI-Box," [Accessed: 26- Nov- 2018]. [Online]. Available: https://static.bhphotovideo.com/lit_files/84886.pdf

[33] J. Butler and C. Sherman, *Transducers and Arrays for Underwater Sound*, ser. Modern Acoustics and Signal Processing. Springer International Publishing, 2016.